Mapping Depth to Argillic Soil Horizons Using Apparent Electrical Conductivity

Kenneth A. Sudduth[1], Newell R. Kitchen[1], D. Brenton Myers[2] and Scott T. Drummond[1]
[1]Cropping Systems and Water Quality Research Unit, USDA Agricultural Research Service, Columbia, MO 65211
Email: Ken.Sudduth@ars.usda.gov
[2]Department of Soil and Water Science, University of Florida, Gainesville, FL 32611

ABSTRACT

Maps of apparent electrical conductivity (EC_a) of the soil profile are widely used in precision agriculture. A number of EC_a sensors are commercially available, each with a unique response function (*i.e.*, the relative contribution of soil at each depth to the integrated EC_a reading). Our past research estimated depth to an argillic horizon (*i.e.*, topsoil depth, TD) on claypan soils by fitting empirical equations to EC_a sensor data. The objective of this research was to determine if TD estimates could be improved by combining data from multiple EC_a sensors and by solving for TD by inverting a two-layer soil model incorporating instrument response functions. Data were obtained with three sensors having five different EC_a depth-response functions (Veris 3150*, Geonics EM38 vertical dipole mode, and DUALEM-2S) on two Missouri claypan-soil fields. Soil cores obtained in each field provided measured TD data for calibration and validation. Using a numerical optimization approach, response-function models were developed for EC_a variables individually and in combination. Similarly, linear regression was applied to single and multiple variables. Root mean square error of validation ($RMSE_v$) of single-variable TD estimates was 22 to 25 cm, with better results for those variables with moderately deep EC_a response functions. Results from the model-based approach were very similar to those obtained by regressing TD on EC_a^{-1}. The best calibrations using multiple variables in model inversion or regression were somewhat better than those using single variables, with $RMSE_v$ of 22 cm and 20 cm, respectively. For all approaches, highest TD errors were localized to one area of one field, possibly because soils in this area violated the model assumption of spatially homogeneous soil layer conductivity. Although these calibrations are sufficiently accurate to be useful in TD mapping, a model solution allowing layer conductivities to vary spatially should be investigated for possible improvements.

Introduction

Efficient and accurate methods of measuring within-field variations in soil properties are important for precision agriculture. Sensors that can collect dense datasets while traversing a field provide several advantages over traditional measurement methods that involve soil sample collection and analysis. These advantages may include lower cost, increased efficiency, and more timely results. In addition, the ability of a sensor to obtain data at many more points, as compared to sampling methods, means that overall spatial estimation accuracy can increase even if the accuracy of individual measurements is lower.

Apparent electrical conductivity (EC_a) of the soil profile is a sensor-based measurement that can provide an indirect indicator of important soil physical and chemical properties. Soil salinity, clay content, cation exchange capacity (CEC), clay mineralogy, soil pore size and distribution, and soil moisture content are some of the factors that affect EC_a (McNeill, 1992). For saline soils, most of the variation in EC_a can be related to salt concentration (Williams and Baker, 1982). In non-saline soils, conductivity variations are primarily a function of soil texture, moisture content, bulk density, and CEC (Corwin and Lesch, 2005). A theoretical basis for the relationship between EC_a and soil properties was developed by Rhoades *et al.* (1989). In this model, EC_a was defined as a function of soil water content, the electrical conductivity of the soil water, soil bulk

* Mention of trade names or commercial products is solely for the purpose of providing specific information and does not imply recommendation or endorsement by the US Department of Agriculture or the University of Florida.

density, and the electrical conductivity of the soil particles. Recently, techniques have been developed to use this model for predicting the expected correlation structure between EC_a data and multiple soil properties of interest (Lesch and Corwin, 2003).

Two types of EC_a sensors are used in agriculture, an electrode-based sensor requiring soil contact and a non-contact electromagnetic induction (EM) sensor. The Veris 3100/3150 (Veris Technologies, Salina, KS) uses six rolling coulters for electrodes and provides two simultaneous EC_a measurements (Lund *et al.*, 1999). The EM38 (Geonics Limited, Mississauga, Ontario, Canada) is a lightweight bar designed to be carried by hand to provide stationary EC_a readings. To implement mobile data acquisition with this unit, it is necessary to assemble a transport mechanism and data collection system (*e.g.*, Sudduth *et al.*, 2001). The EM sensing approach (McNeill, 1992) is also used by the DUALEM sensors (Dualem, Inc., Milton, Ontario, Canada) which provide two or more simultaneous measurements. Each type of EC_a sensor has its own operational advantages and disadvantages (Sudduth *et al.*, 2003).

In addition to estimating levels of the soil properties given above, EC_a has been used to estimate the thickness of soil layers with contrasting conductivities. Our group developed EC_a regressions for the depth of flood-induced sand deposition (Kitchen *et al.*, 1996) and for topsoil depth (TD) above a subsoil argillic horizon (Doolittle *et al.*, 1994; Kitchen *et al.*, 1999; Sudduth *et al.*, 2001; Sudduth *et al.*, 2003). Others have also reported statistical relationships between EC_a and the depth of contrasting soil layers (Bork *et al.*, 1998; Mueller *et al.*, 2003; Cockx *et al.*, 2007).

Researchers have also developed procedures to estimate layer conductivities and thicknesses by inverting theoretical models of EC_a instrument response. In this way, the form of the relationship is defined by the nonlinear theoretical response model, rather than by whatever model might be fit in a statistical solution. Many of these inversion solution approaches (*e.g.*, Hendrickx *et al.*, 2002) require data from an EC_a sensor held at multiple heights above the ground at each sampling point. Practical application of such approaches for mobilized mapping of large areas is therefore limited. Saey *et al.* (2008) used single-height EM38 data in an inversion solution to directly solve for the depth of loess topsoil over clay subsoil. The underlying assumption of this approach was that each soil layer was spatially homogeneous, with a uniform layer EC_a over the study area. At a 2.7-ha test site, a strong nonlinear relationship (r^2 = 0.86) was found between EC_a and loess topsoil depth. Results were confirmed using an independent validation set with a range in topsoil depth of 1.5 m, where a root mean square error (RMSE) of 22 cm was found. In further work on the same test site, Saey *et al.* (2009) investigated two additional model inversion approaches: (1) using the two EC_a channels of an EM38-DD sensor in a solution that also assumed spatial homogeneity of the two soil layers, and (2) using the four EC_a channels of a DUALEM-21S sensor in a solution that allowed variable layer conductivities to be calculated at each measurement point. These two approaches produced equivalent accuracies, with RMSE values of 26 cm. However, the four-channel approach was described as more efficient because it did not require the 56 calibration measurements of TD that were used with the EM38-DD dataset and with the EM38 dataset of Saey *et al.* (2008).

The TD above the argillic horizon is an important factor in soil quality and productivity for the claypan soils of the central U.S.A. (Kitchen *et al.*, 1999). In past research, we estimated this TD by fitting empirical regression equations to single-sensor EC_a data. The objective of this research was to determine if other approaches could improve TD estimates. These other approaches included (1) combining data from multiple EC_a sensors, and (2) solving for TD by inverting a two-layer soil model incorporating EC_a response functions.

Materials and Methods

EC_a Sensors and Response Curves

The Geonics EM38 can be operated in two orientations, vertical dipole and horizontal dipole. The effective measurement depth, above which 70% of the cumulative response occurs, is approximately 1.5 m for the vertical dipole mode and 0.75 m for the horizontal dipole mode (McNeill, 1992). In this research, the EM38 was operated only in the vertical dipole mode. We chose not to use the EM38 horizontal dipole mode because this would have required a second data collection operation. Additionally, because the depth response of the EM38 horizontal reading is between those of the two Veris readings, we expected that little additional information would be obtained. The EC_a measurement from the EM38 vertical dipole mode (designated as $EC_{a\text{-}em}$ in this study) is averaged over a lateral area approximately equal to the measurement depth (McNeill, 1992).

For all EC_a instruments, the theoretical incremental response to soil conductivity varies as a nonlinear function of depth. That is, a soil layer of a given conductivity will affect the measured reading differently, depending on how far away the instrument is from the layer. The form of the response equation varies for different coil configurations. For the EM38 in vertical

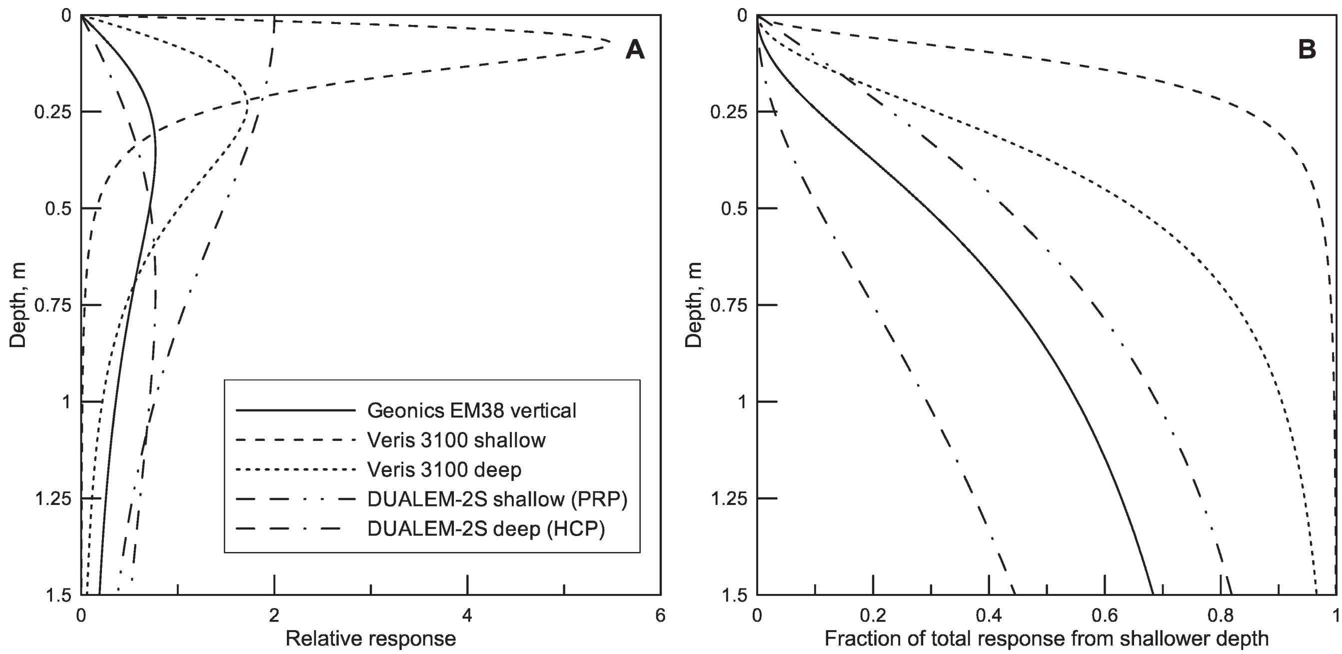

Figure 1. Incremental (a) and cumulative (b) responses of the EC_a sensors used in this study.

dipole mode, where both transmitter and receiver coil windings are horizontal, the response (Φ_{em}) is given by Eq. (1) (McNeill, 1980):

$$\Phi_{em} = 4z\left(4z^2+1\right)^{-3/2}, \tag{1}$$

where z = distance below sensor, m. Sensitivity in the vertical mode is highest at about 0.4 m below the instrument (Fig. 1(A)). The EC_a measurement is an integrated response to soil conductivity with depth, as weighted by this instrument response function (McNeill, 1992). Theoretical considerations underlying the derivation of the instrument response functions are discussed by McNeill (1980).

The DUALEM-2S incorporates a single transmitter and two receivers, simultaneously providing two different depth-weighted estimates of EC_a. The transmitter and one receiver have horizontal windings, forming what is termed a horizontal co-planar (HCP) geometry and giving the deeper of the two readings. The other receiver has vertical windings, forming a perpendicular (PRP) geometry that generates a shallower reading. For the purposes of this report, we refer to the two DUALEM-2S readings as $EC_{a\text{-}Ddp}$ (deep) and $EC_{a\text{-}Dsh}$ (shallow). Using the same definition as for the EM38 above, the manufacturer reports effective sensing depths of 3.0 m and 1.2 m, respectively (Dualem, 2005). The HCP geometry of the DUALEM-2S is the same as used in the EM38 vertical dipole mode, so the theoretical response in that mode (Eq. (2)) varies from Eq. (1) only because of the fact that the coil separation is 2 m rather than the 1 m of the EM38:

$$\Phi_{HCP} = \Phi_{Ddp} = 2z\left(z^2+1\right)^{-3/2}. \tag{2}$$

The response of the DUALEM-2S in the PRP mode, with a 2.1-m coil separation and a different receiver coil orientation, is given by Eq. (3) (Dualem, 2005):

$$\Phi_{PRP} = \Phi_{Dsh} = 2\left(0.907z^2+1\right)^{-3/2}. \tag{3}$$

The Veris 3100 (Lund *et al.*, 1999) and 3150, whose EC_a sensing component is functionally equivalent to the 3100, use rolling coulter electrodes to directly sense both shallow and deep readings of EC_a (designated as $EC_{a\text{-}Vsh}$ and $EC_{a\text{-}Vdp}$, respectively). As with the EM sensors, the Veris response to soil conductivity varies as a nonlinear function of depth. The electrodes of the Veris 3100/3150 are configured in a Wenner array. The theoretical response of the Wenner array (Roy and Apparao, 1971) is given by Eq. (4) for the Veris deep reading and by Eq. (5) for the Veris shallow reading:

$$\Phi_{Vdp} = 5.87z\left(\left(0.538+4z^2\right)^{-3/2} - \left(2.15+4z^2\right)^{-3/2}\right) \tag{4}$$

$$\Phi_{Vsh} = 1.87z\left(\left(0.0544+4z^2\right)^{-3/2} - \left(0.218+4z^2\right)^{-3/2}\right). \tag{5}$$

The graph of these responses (Fig. 1(A)) shows them to be similar in shape to the response of the two EM sensors, although the two Veris responses reach a maximum nearer the soil surface and then decrease more rapidly with depth.

Integrating the response curves with respect to depth gives the cumulative fraction of the total response to depth z (Eqs. (6)–(10)):

$$R_{em} = 1 - \left(4z^2 + 1\right)^{-1/2} \tag{6}$$

$$R_{Ddp} = 1 - \left(z^2 + 1\right)^{-1/2} \tag{7}$$

$$R_{Dsh} = 0.952z\left(0.907z^2 + 1\right)^{-1/2} \tag{8}$$

$$R_{Vdp} = 1 - 11\left(2\left(225z^2 + 121\right)^{1/2} - \left(900z^2 + 121\right)^{1/2}\right) \left(225z^2 + 121\right)^{-1/2}\left(900z^2 + 121\right)^{-1/2} \tag{9}$$

$$R_{Vsh} = 1 - 7\left(2\left(900z^2 + 49\right)^{1/2} - \left(3600z^2 + 49\right)^{1/2}\right) \left(900z^2 + 49\right)^{-1/2}\left(3600z^2 + 49\right)^{-1/2}. \tag{10}$$

The variation between the cumulative response curves (Fig. 1(B)) clearly shows that the different sensors respond to different soil volumes. As an example, consider the depth above which 90% of the response is obtained. With the Veris shallow reading ($EC_{a\text{-}Vsh}$), 90% of the response is obtained from the soil above the 0.3-m depth. For the Veris deep reading ($EC_{a\text{-}Vdp}$), 90% of the response is obtained from the soil above the 1.0-m depth. With the EM38 vertical reading ($EC_{a\text{-}em}$), 90% of the response is obtained above about 5.0 m. With the DUALEM-2S, the 90% threshold is reached at about 2.2 m for $EC_{a\text{-}Dsh}$ and 10 m for $EC_{a\text{-}Ddp}$. The response curves (Fig. 1) are based on equations that assume a homogeneous soil volume. Actual weighting functions will vary somewhat because of EC_a differences among soil layers, with a highly conductive surface layer reducing the response depth (Barker, 1989).

Single-Variable Two-Layer Soil Model

Following McNeill (1980) and Saey *et al.* (2008), we modeled the claypan soil profile as two layers of homogeneously conductive material. Further, because we collected EM38 and DUALEM-2S data with the instruments above the ground on wheeled carts, the overall model consists of three layers, including the air gap between the instrument and the soil. The model (Eq. (11)) gives the instrument reading (EC_{ax}, where x is the instrument designation, *e.g.*, Vdp) as a function of height of the instrument above the ground (HI), EC_a of the topsoil (EC_{aT}), EC_a of the subsoil (EC_{aS}), and topsoil depth (TD):

$$EC_{ax} = \int_0^{HI} EC_{air}\Phi_x(z)\,dz + \int_{HI}^{TD+HI} EC_{aT}\Phi_x(z)\,dz + \int_{TD+HI}^{\infty} EC_{aS}\Phi_x(z)\,dz. \tag{11}$$

Because EC_{aT} and EC_{aS} are assumed constant over their respective depth intervals, and assuming $EC_{air} = 0$, the model can be integrated and expressed in terms of the cumulative response functions (Eq. (12)):

$$EC_{ax} = EC_{aT}\,R_x(TD+HI) - EC_{aT}\,R_x(HI) + EC_{aS}\,R_x(\infty) - EC_{aS}\,R_x(TD+HI). \tag{12}$$

Equation 12 is solved for $R_x(TD + HI)$, and then $z = TD + HI$ is obtained by inverting the appropriate cumulative response (Eqs. (6)–(10)), either analytically or numerically. The two unknown constants EC_{aT} and EC_{aS} are determined iteratively as the values of these two parameters that minimize the RMSE between the calculated TD and measured TD for the points in a calibration dataset, subject to the constraint $TD \geq 0$.

Multiple-Variable Two-Layer Soil Model

We considered two ways of solving a multiple-variable two-layer soil model, following the two approaches given by Saey *et al.* (2009). The models used in the solutions are based on Eq. (12) above, replicated for each EC_a variable included. In the first approach, multiple EC_a datasets are used along with TD calibration point data. The solution proceeds as described above for the single-variable approach, except that the TD error is minimized in a least-squares sense with respect to the TD values calculated from all EC_a datasets included in the analysis. In the second approach, TD calibration data are not used. Rather, the system of response equations (based on one instance of Eq. (12) for each EC_a variable included) is solved simultaneously for TD, EC_{aT}, and EC_{aS}. This requires a minimum of three EC_a variables for an exact solution. If more EC_a variables are included, a least-squares optimized solution is obtained.

Study Fields

Data were collected on two fields (Field 1, 35 ha and Field 2, 13 ha) located within 3 km of each other near Centralia (39° 13′ N, 92° 08′ W), in central Missouri. The fields were managed in a corn-soybean rotation for at least 10 yr prior to data collection, using either minimum-tillage (Field 1) or no-tillage (Field 2). Both fields included a complete range of landscape positions from summit to footslope, but relief on Field 2 (12 m) was greater than on Field 1 (6 m).

The claypan soils found at the study fields were typical of major land resource area (MLRA) 113, the central claypan area (USDA, 1981). The soils are primarily of the Mexico (fine, smectitic, mesic aeric Vertic Epiaqualfs), Adco (fine, smectitic, mesic aeric Vertic Albaqualfs), and Leonard (fine, smectitic, mesic, Vertic Epiaqualfs) series. These soils were formed in moderately-fine textured loess over a fine textured pedisediment and are classified as somewhat poorly drained. Surface textures range from silt loam to silty clay loam. The namesake "claypan" argillic horizon has an abrupt upper boundary with at least 100% more clay than in the horizon above. Texture of this horizon, which commonly contains as much as 50 to 60% smectitic clay is typically classed as silty clay loam, silty clay, or clay. Within each study field, topsoil depth above the claypan (TD, depth to the first B horizon) ranged from less than 10 cm to greater than 100 cm.

Data Collection

The EC_a data for each field were collected over two consecutive days in the fall of 2005. At the time of data collection, soil temperature at an 8 cm depth was approximately 13°C and average soil water content was 27%. The ground surface was moist but trafficable, with about 2 cm of rain having occurred three days previously. The EM38 and DUALEM-2S were combined with a wheeled cart, data acquisition computer, and differential GPS (DGPS) system for mobile data collection, as described by Sudduth *et al.* (2001). Measurements were obtained with the DUALEM-2S on an approximate 10-m transect spacing (Fig. 2). Because of time constraints, the Veris 3150 and Geonics EM38 were operated on transects spaced 20-m apart aligned with every other DUALEM-2S transect. Soil EC_a (mS/m) was recorded on a 1-s interval, corresponding to a 4-m to 6-m data spacing. Data obtained by differential GPS was associated with each sensor reading to provide positional information with an accuracy of 1 m or better. Raw EC_a data were offset by 1 s to compensate for the position of the GPS antenna ahead of the sensor and for time lags in the data acquisition system (Sudduth *et al.*, 2001).

The TD calibration dataset was obtained as part of a previous investigation (Sudduth *et al.*, 2003). The calibration sites (19 in Field 1 and 15 in Field 2; Fig. 2) were chosen to provide EC_a values distributed similarly to those in the EC_a map, with the additional goal of including samples from all the landscape positions and soil map units present in the field. Cores were examined within the field by a skilled soil scientist for TD determination. Identification of the top of the argillic horizon (*i.e.*, TD) was based on a combination of the moist consistency of the soil, resistance to knife

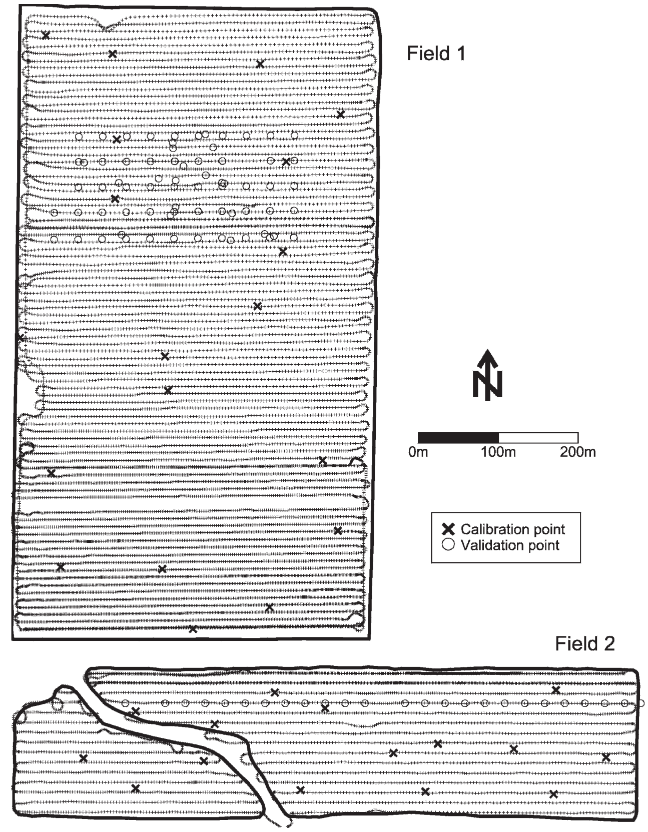

Figure 2. Map of the two study fields with calibration and validation points and DUALEM-2S data collection transects. EM38 and Veris 3150 data were collected along every second transect.

insertion, and gloss of the core surface (Myers *et al.*, 2007). At two of the 34 calibration sites, the increase in clay was not great enough to define an argillic horizon; at these locations TD was taken as the depth to the first layer with notable clay content increase.

Additional locations within the two fields where TD was previously measured using the same procedures, but by other scientists, were used as a validation dataset (Fig. 2). These sites were established by Myers (2005) on Field 1 in a regular grid (n = 70) and by Sudduth *et al.* (2000) on Field 2 as a single transect (n = 25).

Data Analysis

EC_a values corresponding to calibration and validation point locations were extracted from each EC_a dataset by point kriging using GS+ version 5.1.1 (Gamma Design Software, Plainwell, MI). For each EC_a dataset-field combination, the best semivariogram model – exponential or spherical in all cases – was used in kriging. All semivariograms fit the EC_a data very well, with $r^2 \geq 0.98$ and nugget semivariance $\leq$ 15% of total semivariance in all cases.

To implement the model inversion approaches that included TD calibration point data, a Visual Basic program was written. This program determined parameter values and calibration statistics for TD estimation of each field-EC_a dataset combination using Eq. (12) and the appropriate cumulative response function (Eqs. (6)–(10)). Calibrations were also developed for a combined dataset including all points from both fields. Model inversion solutions that did not include TD calibration data were obtained by nonlinear optimization based on Levenberg-Marquardt least squares using the NLPLM subroutine in SAS PROC IML.

In regression we modeled TD as an inverse function of EC_a plus an intercept term. In previous research (Doolittle *et al.*, 1994) we compared several linear and nonlinear equation forms and found an exponential equation to be the best estimator of claypan-soil TD. In a subsequent study (Sudduth *et al.*, 2001) we determined that an exponential equation with an exponent of -1 (*i.e.*, EC_a^{-1}) provided results almost as good as those obtained with the best-fit exponent value. We have used this modeling approach.

This model was implemented as a linear regression on EC_a^{-1} using PROC REG in SAS version 9.1 (SAS Institute, Inc., Cary, N.C.). Statistical analyses combining multiple EC_a^{-1} datasets were carried out using SAS PROC STEPWISE.

Results and Discussion

Single-Variable Model Inversion

The most accurate TD calibrations by model inversion were obtained with $EC_{a\text{-}Dsh}$ (PRP) data (Table 1, Fig. 3). The same trend was seen for each field separately and for both fields combined. With $EC_{a\text{-}Dsh}$ data, model-optimized values of EC_{aT} and EC_{aS} were reasonable, falling within the range of profile EC_a data collected on Field 2 in another project (Sudduth *et al.*, 2000). These layer EC_a values were also reasonable when using data from the EM38, which has a similar depth response (Fig. 1). Accuracies of the $EC_{a\text{-}Ddp}$ calibrations were better than the $EC_{a\text{-}em}$ calibrations for Field 2 and the combined dataset, while $EC_{a\text{-}em}$ calibrations were better for Field 1. However, the $EC_{a\text{-}Ddp}$ calibrations optimized unrealistically, at or near $EC_{aT} = 0$ (Table 1). This dataset is the most strongly weighted to deeper parts of the soil profile, with only about 45% of its cumulative response coming from above 1.5 m (Fig. 1). As determined by coring, the soil profiles on these fields exhibited paleosols (soils that formed in the past and were subsequently buried under new parent material) between 1 and 1.5 m at some, but not all locations, as well as glacial till at approximately 2 to 3 m (unpublished data). As a paleosol or till would likely have EC_a different from other subsoil layers, the presence or absence of these layers could result in spatially variable EC_{aS}, violating model assumptions. Because $EC_{a\text{-}Ddp}$ readings would be most strongly affected by EC_a deep in the profile, results with this dataset would be affected the most. Calibrations with the Veris 3150 datasets also tended toward unrealistically low values for EC_{aT} and higher RMSE (Table 1). The responses of both Veris readings, particularly V_{sh}, are strongly weighted to the surface soil (Fig. 1). Soil profiles in these fields exhibit spatially variable topsoil clay content (CV = 22% for the calibration points in this study), which would also imply spatially variable EC_{aT}, again violating model assumptions. This could have been caused, for example, by tillage mixing of argillic horizons into the more silty topsoil material, especially in soils with small TD. The surface-weighted response of the Veris sensor would make those datasets most susceptible to spatial variation in EC_{aT}.

The relationship of topsoil depth to EC_a^{-1} was stronger for Field 2 than for Field 1 (Fig. 3(A)). While calibration points for Field 2 closely fit an inverse function, the calibration points on Field 1 with measured topsoil depths between 15 and 40 cm exhibited more scatter. In particular, several of the points further removed from the general trend were ones where a paleosol was found through soil coring (circled points in Fig. 3(A)). The presence of this additional layer deep in the profile apparently affected the EC_a-TD relationship. Additionally, the calibration points were not evenly distributed across the EC_a range of interest for Field 1, with only one point having TD above 50 cm. Calibration point selection might be improved using the approach proposed by Lesch *et al.* (1995), who described an algorithm for selecting optimum locations for EC_a calibration points.

The two fields in this study had similar soils and were managed similarly, and the EC_a data for both fields were collected within 4 d and under similar conditions. Because of this similarity and because we desired a general calibration to TD, we pooled data from both fields for further analysis and validation. Although calibration results for Field 2 were considerably worse with the combined dataset, calibration results for Field 1 were similar for combined and field-specific datasets. Performance of the combined-dataset TD model was assessed through application to the combined validation set of measured TD data from both Fields 1 and 2. Similar to calibration results, lowest validation RMSE was obtained using $EC_{a\text{-}Dsh}$, followed by $EC_{a\text{-}Ddp}$ and $EC_{a\text{-}em}$ (Table 1). All models provided results with relatively low bias errors ranging from 4 to 7 cm in this separate validation dataset. As in the calibration results, the largest deviations of $EC_{a\text{-}Dsh}$-estimated TD

Table 1. Parameter values and calibration and validation set statistics for estimation of claypan soil topsoil depth (TD) by inversion of EC_a response profiles and by linear regression on EC_a^{-1}.

		Model inversion solution						Regression solution				
				Calibration		Validation					Validation	
Location	EC_a source	EC_{aT} (mS/m)	EC_{aS} (mS/m)	RMSE (cm)	Bias (cm)	RMSE (cm)	Bias (cm)	b_0*	b_1*	Calib. RMSE (cm)	RMSE (cm)	Bias (cm)
Field 1	$EC_{a\text{-Vsh}}$	0	89	25.7	−0.1	25.1	0.1	27.8	52.4	26.8	25.1	0.4
	$EC_{a\text{-Vdp}}$	0	40	22.5	−0.9	24.4	1.3	5.8	590.8	23.1	23.9	0.1
	$EC_{a\text{-em}}$	18	65	17.3	−0.4	24.2	2.2	−87.8	5,946	18.3	23.6	2.9
	$EC_{a\text{-Dsh}}$	17	66	15.5	0.1	22.2	2.4	−64.6	4,179	15.6	21.8	2.2
	$EC_{a\text{-Ddp}}$	0	70	21.5	−3.3	23.3	2.5	−119	9,681	18.4	22.6	3.8
Field 2	$EC_{a\text{-Vsh}}$	6	112	31.5	1.8	22.8	12.3	−31.2	795.7	30	22.7	10.0
	$EC_{a\text{-Vdp}}$	12	46	22	−9.8	13.8	−2.8	−53	2,835	15.8	19.1	6.6
	$EC_{a\text{-em}}$	20	75	17.6	−0.1	13.3	−5.5	−116.2	8,431	18.5	12.7	−3.6
	$EC_{a\text{-Dsh}}$	25	71	11.4	−0.1	13.4	−3.6	−100.3	6,461	12.7	12.1	−1.7
	$EC_{a\text{-Ddp}}$	1	75	14.4	−1.8	19.7	−6.9	−161.1	12,986	12.7	15.7	−5.0
Combined	$EC_{a\text{-Vsh}}$	0	143	30.8	0	25.3	5.8	31.5	64.1	31.9	25.3	4.6
	$EC_{a\text{-Vdp}}$	0	54	26.6	−0.2	24.9	7.4	8.2	721.8	28.3	24.1	5.6
	$EC_{a\text{-em}}$	18	69	20.9	−1.6	25.1	3.6	−91	6,525	21.2	24.5	5.6
	$EC_{a\text{-Dsh}}$	19	69	17.5	−0.6	22.4	4.1	−76.5	4,979	17.6	21.9	5.0
	$EC_{a\text{-Ddp}}$	0	73	19.7	−0.1	25	5.8	−144.2	11,543	17	22.4	4.2

* b_0 and b_1 are coefficients of the equation $TD = b_0 + b_1(EC_a^{-1})$.

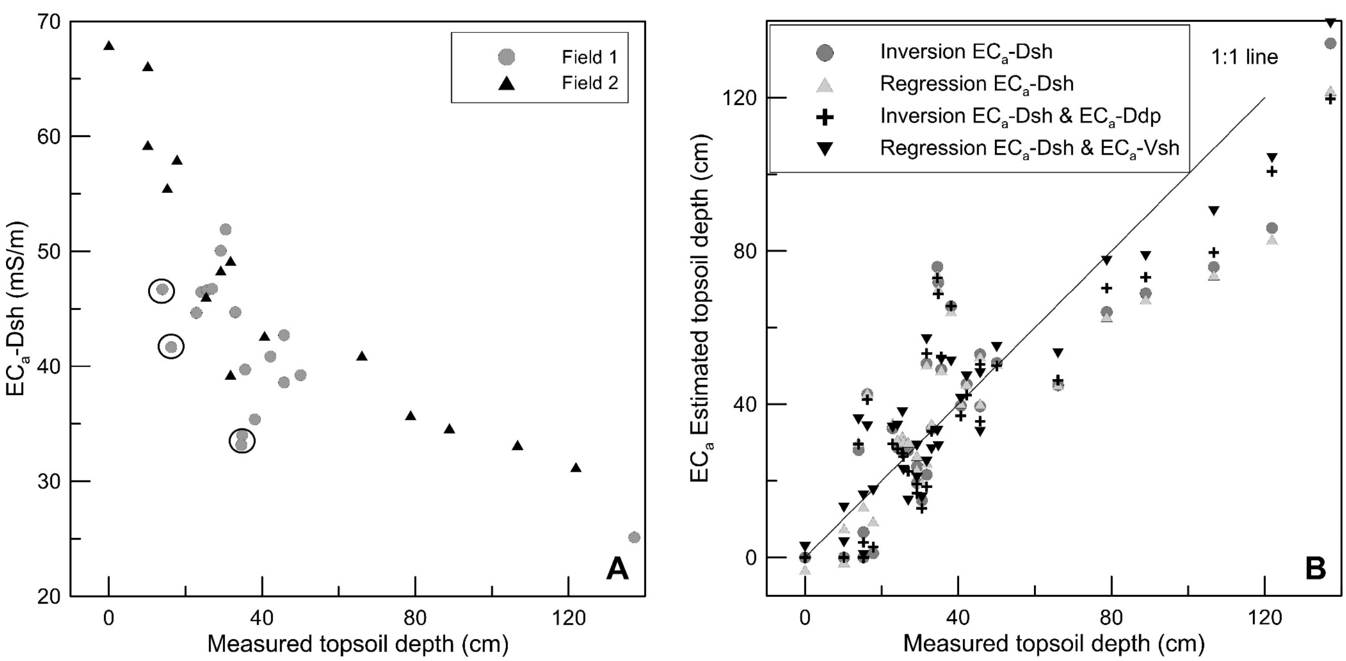

Figure 3. Relationship of $EC_{a\text{-Dsh}}$ reading to measured topsoil depth (a) and calibration set results using inversion and regression methods (b). Calibration points identified as having a paleosol are circled in part a.

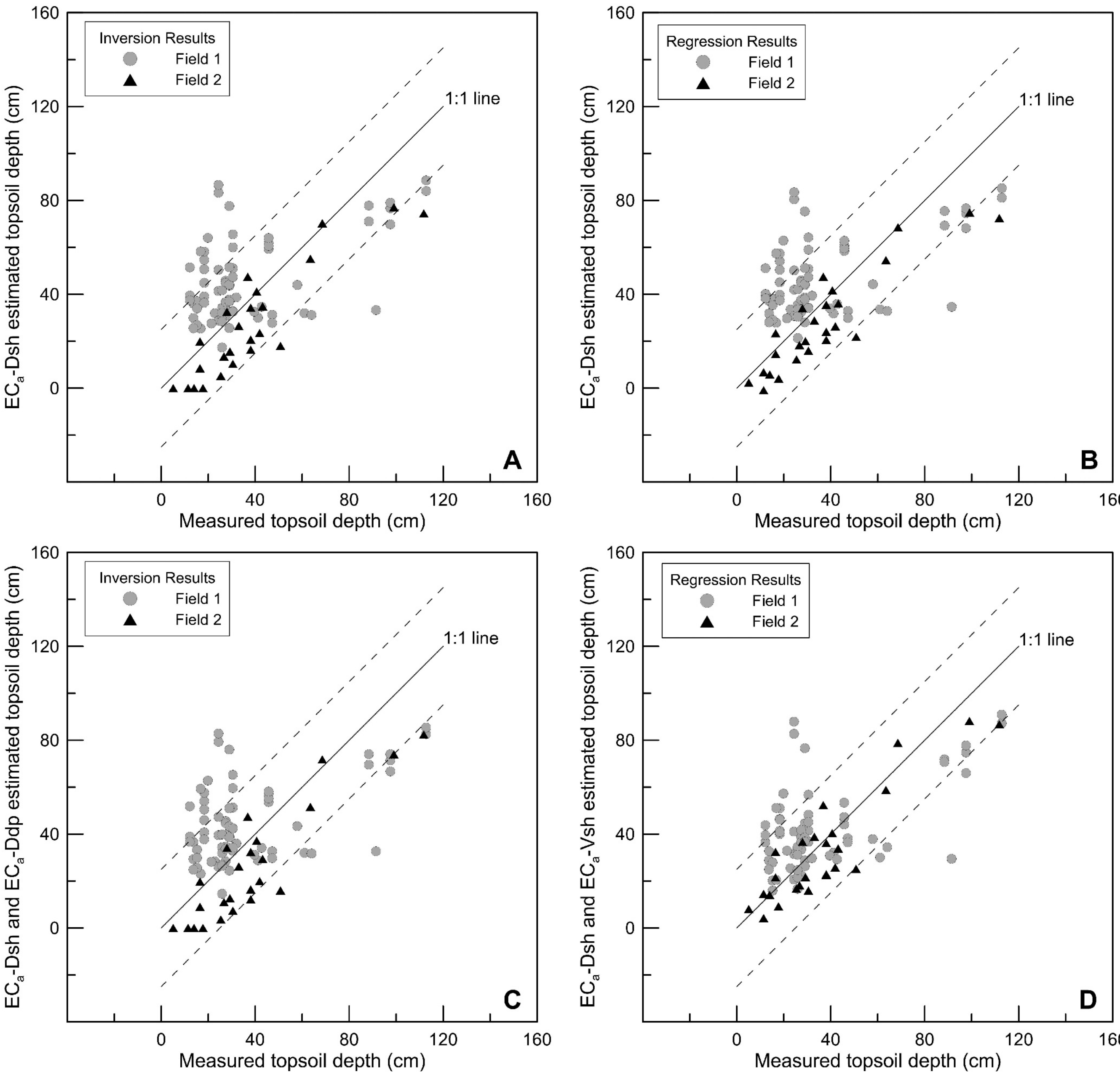

Figure 4. Validation results for most accurate estimations of topsoil depth using single-variable model inversion (a), single-variable regression (b), multiple-variable model inversion (c), and multiple-variable regression (d).

from the 1:1 line were for points with measured TD between 15 and 40 cm (Fig. 4(A)).

Single-Variable Regression

The accuracies of TD estimates by linear regression on EC_a^{-1} (*i.e.*, TD = $b_0 + b_1 EC_a^{-1}$) were very similar to those obtained with the inversion method (Table 1). The $EC_{a\text{-}Dsh}$ reading gave the best results for each field separately, while $EC_{a\text{-}Ddp}$ was only slightly better for the combined dataset. Estimates of TD for individual points in the calibration dataset were very similar between the two methods (Fig. 3(B)). Regression-based results in the validation set were very similar to those obtained by model inversion (Table 1, Fig. 4(B)). We expected the inversion method to perform better, but its accuracy may have been hindered by the required assumption of by-depth uniformity of EC_{aT} and EC_{aS} within the two defined layers. This assumption was violated to a greater or lesser degree at a number of the calibration sites used in this study (Myers, 2008).

Table 2. Calibration and validation set statistics for estimation of claypan soil topsoil depth (TD) by regression on multiple EC_a variables.

Calibration equation	Calibration RMSE (cm)	Validation RMSE (cm)	Validation bias (cm)
$TD = 6{,}755\ EC_{a\text{-}Dsh}^{-1} - 219.3\ EC_{a\text{-}Vsh}^{-1} - 87.65$	11.6	19.8	3.1
$TD = 8{,}254\ EC_{a\text{-}Dsh}^{-1} - 1{,}003\ EC_{a\text{-}Vdp}^{-1} - 108.7$	13.0	19.8	3.3
$TD = 3{,}398\ EC_{a\text{-}Vdp}^{-1} - 827.0\ EC_{a\text{-}Vsh}^{-1} + 3.95$	14.8	23.9	3.3

Multiple-Variable Regression

Stepwise regression analysis included all EC_a^{-1} variables as candidates for entry into the model. Only two EC_a^{-1} terms were statistically significant, with the two best models including the inverse of $EC_{a\text{-}Dsh}$ and either $EC_{a\text{-}Vsh}$ or $EC_{a\text{-}Vdp}$ (Table 2). Figure 3(B) shows that the addition of the Veris reading as a second variable removed much of the scatter in the Field 1 calibration data, compared to single-variable regression or model inversion. However, validation set results with the multiple-variable regression approach (Table 2, Fig. 4(D)) were not much better than the best single-variable results (Table 1). Evidently, calibrations based on two EC_a variables were somewhat prone to overfitting the calibration data, thus reducing validation set performance.

Additional stepwise regressions allowed only the multiple channels within a single instrument (*i.e.*, $EC_{a\text{-}Dsh}$ and $EC_{a\text{-}Ddp}$; $EC_{a\text{-}Vsh}$ and $EC_{a\text{-}Vdp}$) to enter the model. Neither DUALEM-2S channel was statistically significant ($p \geq 0.15$) when both were included in the model, so a two-variable calibration was not appropriate with those data. The calibration with $EC_{a\text{-}Vsh}$ and $EC_{a\text{-}Vdp}$ (Table 2) was better than all single-variable calibrations (Table 1), but validation performance was worse than the two best single-variable calibrations, which used $EC_{a\text{-}Dsh}$ and $EC_{a\text{-}Ddp}$ (Tables 1 and 2).

Multiple-Variable Model Inversion with Calibration Data

The most accurate TD calibration from multiple-variable model inversion was obtained from the two channels of the DUALEM-2S sensor (Table 3, Fig. 3(B)). The accuracy of this calibration was slightly better than that obtained by model inversion with $EC_{a\text{-}Dsh}$ data alone. A calibration that also included $EC_{a\text{-}em}$ along with $EC_{a\text{-}Dsh}$ and $EC_{a\text{-}Ddp}$ gave similar accuracy. The optimized layer conductivity values (Table 3) were reasonable for these calibrations and were similar to those obtained for the best single-variable models (Table 1). Although the best multiple-variable calibration results were better than those with a single variable, best validation results (Fig. 4(C)) were similar between the two approaches (compare Table 3 and Table 1). Both calibration and validation errors were lower with multiple-variable regressions compared to multiple-variable inversions (compare Table 2 and Table 3).

Multiple-variable inversion calibrations that included one Veris channel along with other data were of medium accuracy, while the calibration based on the two Veris channels alone was of lower accuracy. As with the single-variable calibrations described earlier, results with the Veris instrument suffered from its response being too strongly weighted to the surface soil (Fig. 1). Additionally, layer conductivity values obtained with

Table 3. Calibration and validation set statistics for estimation of claypan soil topsoil depth (TD) by inversion of models incorporating multiple EC_a variables.

	Calibration set				Validation set	
EC_a source	EC_{aT} (mS/m)	EC_{aS} (mS/m)	RMSE (cm)	Bias (cm)	RMSE (cm)	Bias (cm)
All variables	33	39	19.7	1.8	23.9	6.6
$EC_{a\text{-}em}$, $EC_{a\text{-}Dsh}$, $EC_{a\text{-}Ddp}$	18	69	17.8	−0.9	23.4	3.4
$EC_{a\text{-}Dsh}$, $EC_{a\text{-}Ddp}$	15	70	16.5	−1.4	22.2	2.7
$EC_{a\text{-}Vsh}$, $EC_{a\text{-}Vdp}$	0	56	26.8	0.6	25	7.7
$EC_{a\text{-}Dsh}$, $EC_{a\text{-}Vsh}$	23	52	19.1	4.1	22	7.5
$EC_{a\text{-}Dsh}$, $EC_{a\text{-}Vdp}$	16	47	23.1	−0.9	25.7	6.1

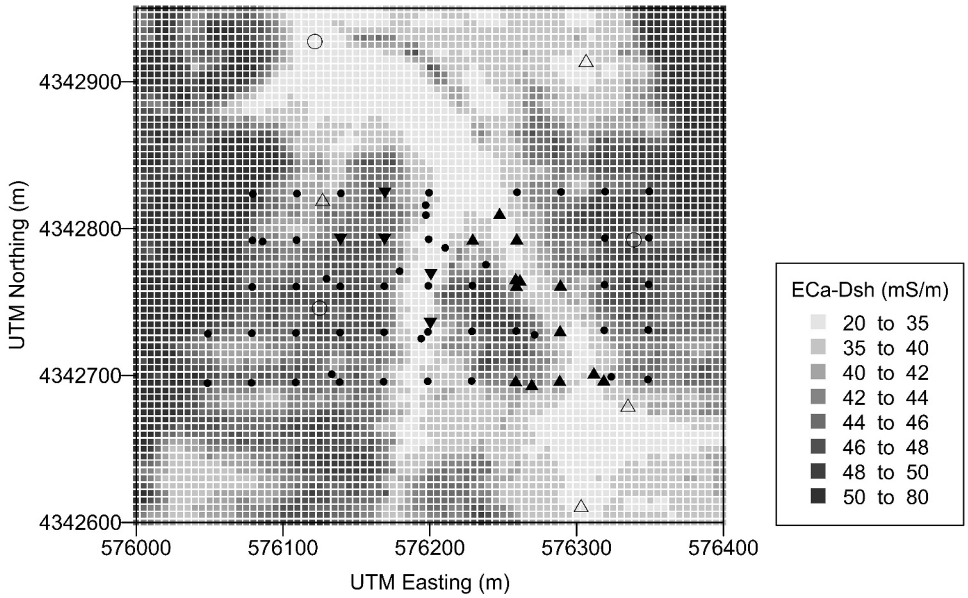

Figure 5. Map of $EC_{a\text{-}Dsh}$ for the portion of Field 1 containing validation points. Upward pointing triangles have TD overestimation (by model inversion using $EC_{a\text{-}Dsh}$) > 25 cm, while downward pointing triangles have TD underestimation > 25 cm. Filled black symbols are validation points, while open black symbols are calibration points.

the Veris calibrations seemed unrealistic in some cases. Investigation of Veris performance under more controlled conditions is needed to resolve this issue.

Multiple-Variable Model Inversion without Calibration Data

This approach yielded unstable results for this claypan-soil TD dataset. Many of the layer conductivities calculated were unreasonably large or small. This is in contrast to results with the same approach reported in Saey *et al.* (2009), where layer EC_a values were noted to be reasonable with relatively small standard deviations ($\leq$21 mS/m). Poor performance in this study could be attributed to the fact that at least three independent EC_a measurements are required to calculate the two layer conductivities and TD at each measurement point. Although five EC_a datasets were available in this study, principal component analysis (PCA) showed that these contained only two statistically independent variables, as two principal components described over 99% of the variance in the dataset. A PCA to verify the presence of the required number of statistically independent EC_a variables would be a useful screening procedure before attempting this type of model inversion analysis.

TD Estimation Accuracy and Limitations

In general, TD estimation results in this study were comparable with those reported in other research. For the dataset containing both fields, the best validation-set RMSE values were 22 cm based on a single EC_a variable and 20 cm based on multiple EC_a variables. Saey *et al.* (2008, 2009) reported validation-set RMSE values from 22 to 26 cm when using different datasets and model inversion approaches. In our work estimating claypan-soil TD (Kitchen *et al.*, 1999; Sudduth *et al.*, 2001; Sudduth *et al.*, 2003), best single-field calibration RMSE values ranged from 6 to 18 cm depending on the specific field. In this study, the lowest field-specific calibration RMSE was 12 cm.

As measured by RMSE, errors in TD using these techniques were on the order of 20 cm. Although this is not a small absolute error, the range in TD on many claypan-soil fields is greater than 100 cm. Thus, these techniques should be sufficient, for example, to divide a field into a few (*i.e.*, 3–5) TD classes for interpretation of crop yield or other response variables. Improved accuracy would be highly desirable for other uses, such as developing input application algorithms based on TD values. Although the calibration techniques used here did a reasonable job of modeling the overall TD-EC_a relationship, improvement may require new approaches that better account for those deviations from the overall relationship that occur from place to place within fields.

In both the model-based and regression-based validation sets, as in the calibration set, there were a few large outliers, mostly from Field 1. Applying the best single-variable inversion calibration ($EC_{a\text{-}Dsh}$) to Field 1, TD was underestimated by more than 25 cm at 7 points and overestimated by more than 25 cm at 11 points. Similar results were obtained from the best calibrations obtained with the other methods examined (Fig. 4). Examination of the $EC_{a\text{-}Dsh}$ map (Fig. 5) for the portion of Field 1 containing the validation points showed that large underestimations of TD (represented by downward pointing triangles in Fig. 5) were generally in areas where EC_a changed significantly over short distances. In these locations, the process of interpolating the EC_a data may not have accurately represented short-range variability, thus causing a lack of correspondence between EC_a and TD data. Additionally, the high topsoil CEC found in that same area of the field (Kitchen *et al.*, 2005) could have increased the EC_{aT} relative to other parts of the field, causing TD to be underestimated.

On the other hand, large overestimations of TD (upward pointing triangles in Fig. 5) had an obvious spatial pattern, following an area of low EC_a that also included calibration points where TD was overestimated by large amounts (Fig. 3(B)). Two linear features of low $EC_{a\text{-}Dsh}$ in Fig. 5 converge into a single linear feature moving from south to north. The feature to the left (west) corresponds to the current drainage channel while the feature on the right appears to be a filled channel. The observed TD for validation points measured within this filled channel is biased by contributions of clay from severely eroded upslope areas. These locations had depositional argillic horizons near the surface while the pedogenic claypan and/or paleosol were deeper in the profile. Topsoil depth was recorded as the depth to the first argillic horizon. These depositional argillic horizons did not have the very high clay content, firm moist consistency, and moderate to strong physical structure seen in claypan horizons and which contributes to increased EC_a (Myers, 2008), and thus led to TD overestimation.

Considering these spatially structured variations in estimation accuracy, it seems reasonable that a modeling approach allowing EC_{aT} and EC_{aS} to vary spatially might provide better TD estimation results. Unfortunately, as described above, this approach was not feasible with the available EC_a data. Collection of data with another sensor, or perhaps by operating one of the existing EM sensors at another height above ground, should be investigated. Additionally, a more complete understanding of how EC_a varies with depth in claypan soils and the effects of mineralogy and soil formation on those variations might improve TD estimation. Layer-based measurements of EC_a as described by Myers (2008) may facilitate further research in this direction.

Conclusions

Inversion of a two-layer soil model using a single EC_a data source successfully estimated topsoil depth variations on claypan-soil fields in central Missouri. Most accurate results were obtained with those EC_a sensors having a moderately deep response function. Inversion estimates were of similar accuracy to those obtained from linear regression using EC_a^{-1} as the independent variable. In terms of validation RMSE, accuracy improvements with model inversions and regressions incorporating multiple EC_a terms were less than 10% when compared to those using a single variable. Multiple-variable inversion solutions were slightly better than multiple-variable regression results, perhaps because the models based on instrument response functions provided a non-linear combination of multiple EC_a data that was more physically accurate than the linear combination provided by multiple linear regression on EC_a^{-1} terms. Estimation errors in a validation set exhibited a spatial structure that appeared to be related to variations in soil properties known to affect EC_a, such as CEC or clay content. A model solution that allows layer conductivities to vary spatially, rather than being constrained to be spatially homogeneous, should be pursued as a potential approach for improved TD estimation.

References

Barker, R.D., 1989, Depth of investigation of collinear symmetrical four-electrode arrays: Geophysics, **54**, 1031–1037.

Bork, E.W., West, N.E., Doolittle, J.A., and Boettinger, J.L., 1998, Soil depth assessment of sagebrush grazing treatments using electromagnetic induction: Journal of Range Management, **51**, 469–474.

Cockx, L., Van Meirvenne, M., and De Vos, B., 2007, Using the EM38DD soil sensor to delineate clay lenses in a sandy forest soil: Soil Science Society of America Journal, **71**, 1314–1322.

Corwin, D.L., and Lesch, S.M., 2005, Apparent soil electrical conductivity measurements in agriculture: Computers and Electronics in Agriculture, **46**, 11–43.

Doolittle, J.A., Sudduth, K.A., Kitchen, N.R., and Indorante, S.J., 1994, Estimating depths to claypans using electromagnetic induction methods: Journal of Soil and Water Conservation, **49**, 572–575.

Dualem, Inc., 2005, DUALEM-1S and DUALEM-2S user's manual, Dualem, Inc., Milton, Ontario.

Hendrickx, J.M.H., Borchers, B., Corwin, D.L., Lesch, S.M., Hilgendorf, A.C., and Schlue, J., 2002, Inversion of soil conductivity profiles from electromagnetic induction measurements: Theory and experimental verification: Soil Science Society of America Journal, **66**, 673–685.

Kitchen, N.R., Sudduth, K.A., and Drummond, S.T., 1996, Mapping of sand deposition from 1993 Midwest floods with electromagnetic induction measurements: Journal of Soil and Water Conservation, **51**, 336–340.

Kitchen, N.R., Sudduth, K.A., and Drummond, S.T., 1999, Soil electrical conductivity as a crop productivity measure for claypan soils: Journal of Production Agriculture, **12**, 607–617.

Kitchen, N.R., Sudduth, K.A., Myers, D.B., Massey, R.E., Sadler, E.J., Lerch, R.N., Hummel, J.W., and Palm, H.L., 2005, Development of a conservation-oriented precision agriculture system: Crop production assessment and plan implementation: Journal of Soil and Water Conservation, **60**, 421–430.

Lesch, S.M., and Corwin, D.L., 2003, Using the dual-pathway parallel conductance model to determine how different soil properties influence conductivity survey data: Agronomy Journal, **95**, 365–379.

Lesch, S.M., Strauss, D.J., and Rhoades, J.D., 1995, Spatial prediction of soil salinity using electromagnetic induction techniques: II. An efficient spatial sampling algorithm suitable for multiple linear regression model identification and estimation: Water Resources Research, **31**, 87–398.

Lund, E.D., Christy, C.D., and Drummond, P.E., 1999, Practical applications of soil electrical conductivity mapping *in* Precision Agriculture '99, Proc. 2nd European Conf. on Precision Agriculture, Stafford, J.V. (ed.), Sheffield Academic Press Ltd., Sheffield, UK, 771–779.

McNeill, J.D., 1980. Electromagnetic terrain conductivity measurement at low induction numbers, Tech. Note TN-6: Geonics Ltd., Mississauga, Ontario.

McNeill, J.D., 1992, Rapid, accurate mapping of soil salinity by electromagnetic ground conductivity meters *in* Advances in Measurement of Soil Physical Properties: Bringing Theory Into Practice, Spec. Pub. 30, Soil Science Society of America, Madison, Wisconsin, 209–229.

Mueller, T.G., Hartsock, N.J., Stombaugh, T.S., Shearer, S.A., Cornelius, P.L., and Barnhisel, R.I., 2003, Soil electrical conductivity map variability in limestone soils overlain by loess: Agronomy Journal, **95**, 496–507.

Myers, D.B., 2005, Soybean root distribution in claypan soils: M.Sc. thesis, University of Missouri, Columbia, Missouri.

Myers, D.B., 2008. Methods for high-resolution soil-landscape modeling in Midwest upland landscapes: Ph.D. dissertation, University of Missouri, Columbia, Missouri.

Myers, D.B., Kitchen, N.R., Sudduth, K.A., Sharp, R.E., and Miles, R.J., 2007, Soybean root distribution related to claypan soil properties and apparent soil electrical conductivity: Crop Science, **47**, 1498–1509.

Rhoades, J.D., Manteghi, N.A., Shrouse, P.J., and Alves, W.J., 1989, Soil electrical conductivity and soil salinity: New formulations and calibrations: Soil Science Society of America Journal, **53**, 433–439.

Roy, A., and Apparao, A., 1971, Depth of investigation in direct current methods: Geophysics, **36**, 943–959.

Saey, T., Simpson, D., Vitharana, U.W.A., Vermeersch, H., Vermang, J., and Van Meirvenne, M., 2008, Reconstructing the paleotopography between the loess cover with the aid of an electromagnetic induction sensor: Catena, **74**, 58–64.

Saey, T., Simpson, D., Vermeersch, H., Cockx, L., and Van Meirvenne, M., 2009, Comparing the EM38DD and DUALEM-21S sensors for depth-to-clay mapping: Soil Science Society of America Journal, **73**, 7–12.

Sudduth, K.A., Hummel, J.W., Kitchen, N.R., and Drummond, S.T., 2000, Evaluation of a soil conductivity sensing penetrometer *in* 2000 ASAE Annual International Meeting Technical Papers (cdrom), Paper No. 001043, American Society of Agricultural Engineers, St. Joseph, Michigan.

Sudduth, K.A., Drummond, S.T., and Kitchen, N.R., 2001, Accuracy issues in electromagnetic induction sensing of soil electrical conductivity for precision agriculture: Computers and Electronics in Agriculture, **31**, 239–264.

Sudduth, K.A., Kitchen, N.R., Bollero, G.A., Bullock, D.G., and Wiebold, W.J., 2003, Comparison of electromagnetic induction and direct sensing of soil electrical conductivity: Agronomy Journal, **95**, 472–482.

U.S. Department of Agriculture, 1981, Land resource regions and major land resource areas of the United States, USDA-SCS Agricultural Handbook 296: U.S. Government Printing Office, Washington, DC.

Williams, B.G., and Baker, G.C., 1982, An electromagnetic induction technique for reconnaissance surveys of soil salinity hazards: Australian Journal of Soil Research, **20**, 107–118.